

ARTICLE OPEN



Degradation of water soluble poly(vinyl alcohol) with acoustic and hydrodynamic cavitation: laying foundations for microplastics

Martin Petkovšek¹, Andrej Kržan², Alenka Šmid³, Ema Žagar² and Mojca Zupanc¹

Water-soluble poly(vinyl alcohol) (PVOH) is widely used in the textile and paper industries and in households as detergent pods. In addition to conventional microplastics, water-soluble PVOH poses an environmental threat because it is usually washed down the drain unnoticed and unobstructed. If not treated during wastewater treatment, it enters the aquatic ecosystem in estimated quantities of several thousand tons annually. The present study aims to address the degradation of PVOH on a laboratory scale by acoustic and hydrodynamic cavitation, assisted or not with an oxidative agent. A hydrodynamic cavitation generator, designed with consideration for real-life application, presents an innovative technology adapted for wastewater treatment. The effects of temperature, addition of external oxidant, and methanol as a hydroxyl radical ($\cdot\text{OH}$) scavenger to PVOH solutions were systematically studied. At optimal operating conditions, PVOH molar mass averages significantly decreased (from weight average molar mass of 124 to 1.6 kg mol⁻¹ in case of 60 min treatment with hydrodynamic cavitation and addition of external oxidant) with concomitant narrowing of molar mass distribution. The SEC/MALS, FTIR, and ¹H NMR results show that mechanical degradation of PVOH chains predominates in acoustic cavitation, while chemical effects also play an important role in hydrodynamic cavitation. Findings from this study could serve as model research for the degradation of other carbon-backbone polymers and provide a route to improved ultimate (bio)degradation of functionalized polymers in the environment.

npj Clean Water (2023)6:35; <https://doi.org/10.1038/s41545-023-00248-8>

INTRODUCTION

Plastic pollution has become the subject of significant scientific attention. This is due to the now apparent ubiquity of plastics in the environment^{1–3}, their large and increasing quantities⁴, the diversity of sources⁵, the types of materials⁶, and the largely unknown fate and long-term effects^{7,8}. Concern has shifted from the initial interest in macro plastic litter, to all forms of microplastics and the current “search” for nanoplastics - particles smaller than 1 μm ranging into the nanometer scale⁹.

The same concerns should apply to water-soluble synthetic polymers, especially full carbon-backbone polymers. Their solubility makes them invisible, however they can persist in the environment and cause unwanted consequences¹⁰. As the most extensively used water-soluble polymer, polyvinyl alcohol (PVOH) is a major cause for such concern¹¹. PVOH is produced through hydrolysis of polyvinyl acetate. Depending on the conditions applied, the hydrolysis reaction may proceed to different degrees, resulting in a copolymer with different content of residual vinyl acetate repeating units, which significantly affect the water-solubility of the copolymer. PVOH with a degree of hydrolysis greater than about 87% is water soluble. PVOH production is estimated at more than 700,000 tons annually and is widely used in food packaging, paper and textile production, construction, adhesives, and medical/pharmaceutical applications¹². Since its introduction in 2012, PVOH has found its way into many households in the form of laundry and dishwashing pods in which a pouch made of PVOH contains the detergent. A recent report by Rolsky and Kelkar¹³ suggests that a large part of PVOH used in detergent pods passes wastewater treatment plants

(WWTP) unchanged with total emissions from this source reaching 7000 tons annually in the US alone. As reported by Hamad et al.¹⁴, PVOH is abundant in wastewater (WW) effluents and can leach from soil into groundwater while mobilizing heavy metals into water streams, making it additionally harmful. As global industrial demand is geared toward greater consumption of polymers, concentrations of these substances in the environment will only increase.

Many efforts are currently directed towards lowering the production, use and consequently pollution with synthetic polymers, however also ways to diminish its amount when already in the environment need to be investigated. WWTP, as the last barrier of defence, presents such an opportunity for the WW pathway¹⁵. Contemporary conventional WWTPs are not capable of effectively capturing microplastics and degrading soluble synthetic polymers, thus appropriate alternative techniques are needed to improve conventional treatment processes¹⁶. An attractive approach to reducing pollution with soluble polymers is to upgrade wastewater treatment (WWT) with techniques that can degrade the polymers to low molar mass intermediates that can be more easily (bio)degraded, thereby reducing the persistence of the polymers in the environment. A study by Alonso-Lopez et al.¹⁷ showed that biodegradation of PVOH under marine conditions without an acclimated inoculum is negligible. Currently the effects of long-term, low concentration exposure to PVOH, are not well understood⁸. Over the years, enough data have been collected to confirm that advanced oxidation processes (AOPs), where $\cdot\text{OH}$ are formed in situ, are very efficient at oxidising many hazardous pollutants in water matrices of varying complexity^{18–20}. In recent years studies investigating degradation of PVOH with

¹Faculty of Mechanical Engineering, University of Ljubljana, Ljubljana, Slovenia. ²Department of Polymer Chemistry and Technology, National Institute of Chemistry, Ljubljana, Slovenia. ³Faculty of Pharmacy, University of Ljubljana, Ljubljana, Slovenia. ✉email: ema.zagar@ki.si; mojca.zupanc@fs.uni-lj.si

various AOPs such as UV/H₂O₂¹⁴, catalytic ozonation²¹ and the Fenton process²² are increasing. The review of Sun et al.²³ concluded that AOPs can effectively degrade PVOH, and that addition of catalysts or an external oxidant can enhance the process. One of AOPs is also cavitation, which, as a physical phenomenon, encompasses growth and collapse of small vaporous bubbles within the liquid due to local pressure drop. When the bubbles collapse, energy is released over a very small spatiotemporal region which drives the mechanical and chemical effects associated with cavitation²⁴. Mechanical effects include high temperatures (reaching several 1000 K)²⁵, local shear forces²⁶, microjets (impinging jet velocities of several 100 m/s)²⁷, and shock waves (several MPa)²⁸, while chemical effects are usually associated with formation of (predominantly) •OH radicals²⁴.

In general, a local pressure drop can result from acoustic waves propagating through the liquid (acoustic cavitation - AC) or from a local increase in velocity via a constriction within the flow (hydrodynamic cavitation - HC)²⁹. In the case of AC, the formation of cavities is confined to a small region, in the vicinity of the low-pressure zones and is therefore suitable for transferring higher energy densities into small volumes. AC is usually generated by piezoelectric elements mounted in ultrasonic baths or ultrasonic horns with excitation frequencies between 20 kHz and 3.2 MHz³⁰. On the other hand, HC is better suited to treat larger volumes of liquids with lower energy input. Among the most commonly studied HC devices are rotational cavitation devices, where the relative motion of the rotor and stator geometry creates the necessary conditions for cavitation to occur. HC has advantages over AC in terms of scalability, energy efficiency, and robustness for WWT applications^{31–33}. As highlighted by Sun et al.²³ and Dong et al.³⁴, there is currently a great need to develop novel methods for WWT that are energy efficient, scalable, and environmentally friendly, with minimal use of external oxidants to effectively destroy a broad range of different pollutants, including microplastics and soluble synthetic polymers such as PVOH. The

advantage of cavitation compared to other AOPs is the simultaneous exploitation of chemical and mechanical effects, thus offering high potential for the degradation of various soluble polymers³⁵. State-of-the-art studies dealing with the effect of cavitation on PVOH degradation are based solely on AC^{23,36–38}, however, differences in the initial PVOH concentration, its molar mass and analytical tools (intrinsic viscosity or molar mass characteristics measurements) used to determine the efficiency of PVOH degradation, makes comparison of the results between these studies^{23,36–38} very difficult. On the other hand, to the author's knowledge, no studies investigating the degradation of PVOH by HC have been reported, thus its effectiveness is yet to be determined.

The objective of this study is therefore to advance the state-of-the-art and to determine and compare the effects of AC and HC on the (pre)degradation of the water-soluble synthetic PVOH polymer. The effects of time, temperature, and the addition of external oxidants on the degradation of PVOH in distilled water were systematically investigated by measuring the molar mass characteristics of PVOH using size-exclusion chromatography coupled to a multi-angle light scattering and refractive index detectors (SEC/MALS-RI), while FTIR and ¹H NMR analyses were used to evaluate the chemical effects of cavitation on PVOH degradation.

RESULTS

Degradation of PVOH followed by measuring its molar mass characteristics by SEC/MALS-RI

PVOH in aqueous solutions was degraded with AC or HC at different experimental conditions listed in Table 1. The degradation of PVOH was followed by measuring its molar mass characteristics using SEC/MALS-RI. Results of PVOH degradation treated at different experimental conditions for 30 min are

Table 1. Overview of experiments, experimental conditions and analysis performed during this study.

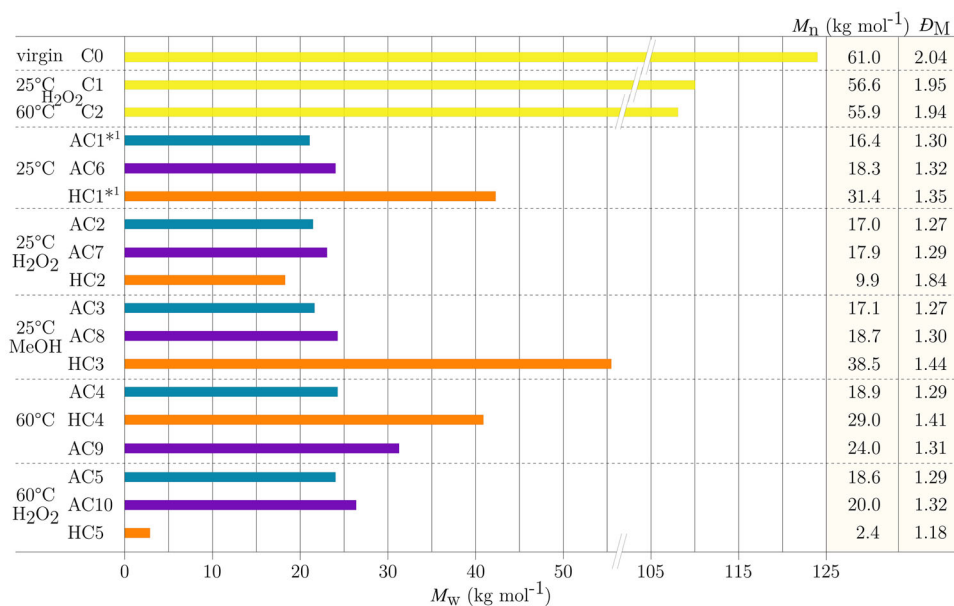
Exp.	Treatment	<i>c</i> (g L ⁻¹)	<i>V</i> (mL)	<i>T</i> (°C)	Additive	Time (min)	MMA \bar{M}_w	FTIR	ACC ^c	ER (Wh L ⁻¹)
C0	—	1	100	—	—	—	x	—	—	—
C1				25	H ₂ O ₂	left overnight	x	—	—	—
C2				60	H ₂ O ₂		x	—	—	—
AC1 ^{*,a} / AC1_t	AC	1	50	25	—	30^a / 5, 15, 30, 60	x	—	x	x
AC2 / AC2_t					H ₂ O ₂	30 / 5, 15, 30, 60	x	—	x	x
AC3					MeOH	30	x	—	—	—
AC4 / AC4_t				60	—	30 / 5, 15, 30, 60	x	—	x	x
AC5 / AC5_t					H ₂ O ₂	30 / 5, 15, 30, 60	x	—	x	x
AC6		2	50	25	—	30	x	—	—	—
AC7					H ₂ O ₂		x	x	—	—
AC8					MeOH		x	—	—	—
AC9				60	—		x	—	—	—
AC10					H ₂ O ₂		x	—	—	—
HC1 ^{*,a} / HC1_t	HC	1	200	25	—	30^a / 5, 15, 30, 60	x	x	x ^b	x
HC2 / HC2_t					H ₂ O ₂	30 / 5, 15, 30, 60	x	x	x ^b	x
HC3					MeOH	30	x	—	—	—
HC4				60	—	30	x	x	x ^b	—
HC5 / HC5_t					H ₂ O ₂	30 / 5, 15, 30, 60	x	x	x ^b	x

Experiments in bold letters are time dependent experiments.

^ameasurements of salicylic acid (SA) products.

^bmeasurements performed in the Venturi microchannel.

^cACC additional cavitation characterisation.



¹ salicylic acid (SA) products formed: 0.59 $\mu\text{g mL}^{-1}$ for AC and 0.50 $\mu\text{g mL}^{-1}$ for HC. These experiments were performed separately, but at the same experimental conditions.

Fig. 1 Molar mass characteristics (M_w , M_n , \bar{D}_M) of PVOH after 30 min treatment with AC or HC cavitation under different experimental conditions (PVOH concentration, temperature, H₂O₂ or MeOH addition). Yellow color bars represent M_w of non-cavitated virgin and control samples; blue and violet color bars represent M_w after AC treatment of PVOH solutions with two concentrations: 1 and 2 g L⁻¹, respectively; and orange color bars represent M_w after HC treatment of PVOH solutions with a concentration of 1 g L⁻¹. Right columns show the corresponding M_n and \bar{D}_M values.

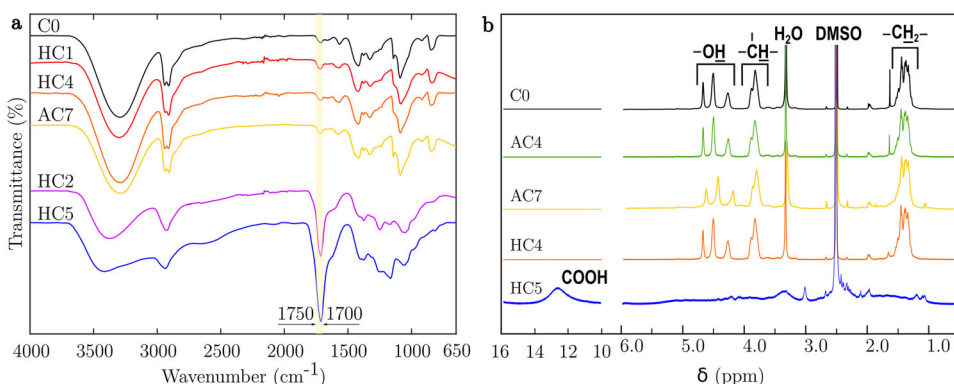


Fig. 2 FTIR and ¹H NMR spectroscopy. (a) FTIR spectra of virgin PVOH (C0) and PVOH samples treated with HC (HC1, HC2, HC4, HC5) and AC (AC7). The carbonyl band (marked yellow) confirms the presence of the aldehyde, ketone, or carboxyl functional groups in the PVOH structure, resulting from oxidation and main chain scission; (b) ¹H NMR spectra of virgin PVOH (C0) and PVOH samples treated with HC (HC4 and HC5) and AC (AC4 and AC7).

presented in Fig. 1, while time dependent experiments (up to 60 min) are presented in Figs. 2 and 3.

Virgin PVOH (Fig. 1: C0) has weight-average (M_w) and number-average (M_n) molar masses of $124 \pm 3 \text{ kg mol}^{-1}$ and $61 \pm 5 \text{ kg mol}^{-1}$, respectively, and dispersity ($\bar{D}_M = M_w/M_n$) of 2.04 ± 0.10 (three parallel prepared solutions). Control experiments where H₂O₂ was added to PVOH solutions, which were treated at RT and 60 °C for 30 min (Fig. 1: C1 and C2) gave slightly lower molar mass averages (MMA) values than virgin PVOH, indicating a certain degree of degradation of PVOH chains in the presence of an external oxidant. Much higher degree of PVOH degradation was observed when solutions were treated with AC or HC regardless of the experimental conditions used (Fig. 1). The MMA and dispersities of the AC treated PVOH do not differ significantly when temperature was increased to 60 °C or when H₂O₂ or MeOH were added, except in the case of AC9. Slight difference can be

seen only among the two different PVOH solution concentrations (1 and 2 g L⁻¹), where lower MMA and \bar{D}_M were obtained with the lower concentration and lower temperature. On the other hand, the MMA and dispersities of the HC treated PVOH solutions with a concentration of 1 g L⁻¹ showed a higher variation between different experimental conditions used. The results show that temperature does not play an important role in the PVOH degradation (Fig. 1: HC1 and HC4), while more efficient PVOH degradation was always achieved with the addition of H₂O₂ (Fig. 1: HC2 and HC5). At 25 °C, PVOH degraded to a lesser extent when MeOH as a radical scavenger (Fig. 1: HC3) was added, indicating that [•]OH formed in HC have a more prominent role than in AC. Furthermore, a clear difference is observed between experiments HC2 and HC5, where in the presence of H₂O₂ a higher temperature considerably increases the degree of PVOH degradation, as shown by the M_w , which decreased to a value of 2.8 kg mol⁻¹ (Fig. 1: HC5).

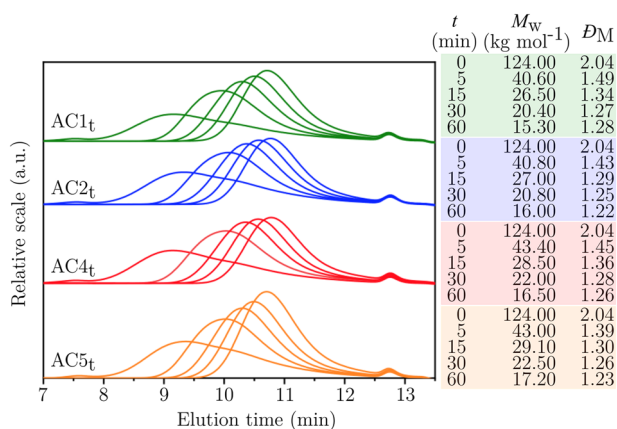


Fig. 3 SEC-RI chromatograms of AC treated PVOH samples - time dependent cavitation treatments. Each colour series shows SEC-RI chromatograms obtained after 0, 5, 15, 30 and 60 min (left to right). Conditions applied: AC1_t (25 °C), AC2_t (25 °C + H₂O₂), AC4_t (60 °C), AC5_t (60 °C + H₂O₂). Right columns show treatment time t , M_w and D_M .

Figure 2a shows FTIR spectra of virgin PVOH and selected PVOH samples treated with AC and HC. In the FTIR spectra of the highly degraded PVOH samples (HC2 and HC5), which show the lowest MMA after HC treatment in the presence of H₂O₂, the intensities of the bands due to the O–H and C–O stretching vibrations at 3400 cm⁻¹ and 1091 cm⁻¹, respectively, decreased significantly, and a new band characteristic of the stretching vibration of the carbonyl group either in the aldehyde, ketone, or carboxyl functional groups appeared in the 1590–1800 cm⁻¹ range^{21,34}. It is significant to note that the FTIR spectra of samples HC1 and HC4 with M_w of approx. 40 kg mol⁻¹, which were also treated with HC but without an external oxidant, show neither an increased intensity of the band for the carbonyl group nor a decrease in the intensities of the O–H and C–H bands. These changes were also not observed in the FTIR spectra of the samples treated with AC in the presence of H₂O₂ (an example is given for AC7).

To further elucidate the degradation mechanism of PVOH, ¹H NMR spectra (Fig. 2b) of the selected samples were also recorded. The ¹H NMR spectrum of virgin PVOH shows signals in the regions of δ 1.1–1.8 ppm and 3.7–4.0 ppm, which originate from the methylene and methyne groups in the main chain, respectively. Three signals appearing between δ 4.2 and 4.8 ppm correspond to the hydroxyl groups in different triad sequences. The methyl group of the residual vinyl acetate repeating units shows a low intensity signal at δ 1.98 ppm because the degree of hydrolysis of the acetate group is high (98%). ¹H NMR spectra of AC or HC-treated PVOH solutions in the absence of H₂O₂ show, in addition to the typical signals of PVOH, the low intensity signals at δ 1.05 ppm (methyl) and 5.89 ppm (allyl), which most likely correspond to the terminal groups originating from the backbone cleavage (HC4 in Fig. 2b), and an unknown signal at δ 8.48 ppm³⁹. All PVOH samples treated with H₂O₂ show additional low intensity signals originating from PVOH oxidation; signals in the range of δ 5.8–5.4 ppm correspond to C = C double bonds, signals at δ 1.86 and 2.09 ppm to newly appearing terminal carbonyl methyl due to backbone cleavage³⁹, and unknown signals at δ 6.2 and 4.1 ppm. Compared to the ¹H NMR spectra of virgin PVOH (C0), PVOH treated with HC in the absence of H₂O₂, and all PVOH samples treated with AC, the ¹H NMR spectra of the highly degraded PVOH treated with HC in the presence of H₂O₂ (samples HC2 and HC5) are very complex and not at all typical of PVOH. Nevertheless, the ¹H NMR spectra of HC2 and HC5 show a broad signal in the range of 12–13 ppm, which is typical for carboxyl groups and thus indicates a high degree of PVOH oxidation (HC5 in Fig. 2b).

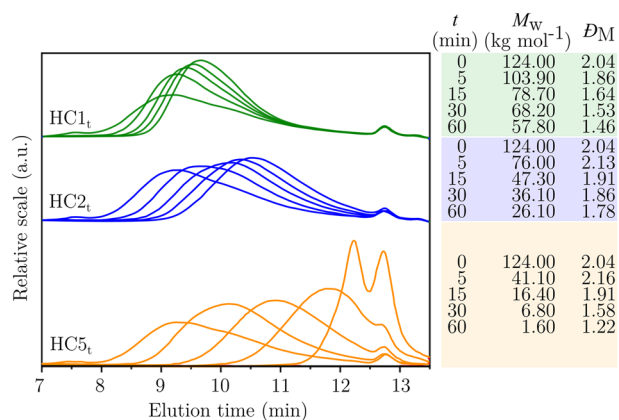


Fig. 4 SEC-RI chromatograms of HC treated PVOH samples - time dependent cavitation treatments. Each colour series shows SEC-RI chromatograms obtained after 0, 5, 15, 30 and 60 min (left to right). Conditions applied: HC1_t (25 °C), HC2_t (25 °C + H₂O₂), HC5_t (60 °C + H₂O₂). Right columns show treatment time t , M_w and D_M .

To investigate the process of PVOH degradation in more detail, an additional set of time-dependent experiments was performed under experimental conditions, the results of which indicated important effects of cavitation. Four experimental conditions (Table 1: AC1_t, AC2_t, AC4_t, and AC5_t) were selected for AC, and three experimental conditions (Table 1: HC1_t, HC2_t and HC5_t) were selected for HC. With prolonged cavitation time, the SEC-RI curves (Figs. 3 and 4) exhibit a gradual shift towards higher elution times, indicating a decrease in MMA with cavitation time. The exponential decrease in the PVOH weight-average molar mass shows that the effect of AC was strongest in the first 5 min of treatment and decreased in the remaining 60 min (Fig. 3). From an initial 124 kg mol⁻¹, the M_w of PVOH decreased to about 40 kg mol⁻¹, while it decreased by only another 19% (from 40 to about 16 kg mol⁻¹) in the remaining 55 min. The plots (Fig. 3) show only slight variations between the four experiments, suggesting that mechanical effects, i.e., shear forces during AC treatment, have a much greater influence on PVOH degradation than chemical effects (·OH generated during AC and addition of H₂O₂). This conclusion is supported by the narrowing of the molar mass distribution reflected by decreasing dispersity, indicating that PVOH chains with higher molar masses are more susceptible to degradation by shear forces than those with lower molar masses, as expected (Fig. 3).

On the other hand, the SEC-RI curves of PVOH samples treated with HC (Fig. 4) show significant differences between the three selected experiments. The time-dependent decrease in M_w confirms the trends obtained in the 30-minutes experiments (Fig. 1). It can be seen that in the case of HC, increasing the cavitation time, increasing the temperature, and adding H₂O₂ enhance the PVOH degradation. The most degraded sample was obtained at 60 min, 60 °C and addition of H₂O₂ (Fig. 4 – case HC5_t). It shows a bimodal distribution with a final M_w of 1.6 kg mol⁻¹. In these experiments, the molecular weight distribution does not narrow as significantly as in the case of AC, indicating that the degradation is also due to chemical effects.

Energy input comparison between the selected time dependent AC and HC experiments

Figure 5 shows a comparison of AC and HC PVOH treatment results in terms of energy consumption. The comparison illustrates that the energy input per sample volume for the same treatment time was higher in case of HC. In terms of energy consumption AC achieved higher degradation rate of PVOH at 25 °C with or without H₂O₂. The highest energy efficiency however was achieved in HC

treatment at elevated temperature and addition of H_2O_2 . As seen in Fig. 3, variations between AC treatment conditions seem to be minor in terms of efficacy, as well as for energy consumption comparison (Fig. 5). On the other hand, variations in HC treatment conditions have an important effect on the efficacy and efficiency, Figs. 4 and 5 respectively.

Characterization of cavitation in distilled water

To better understand the differences between the AC and HC, high-speed visualization was performed in distilled water. Fig. 6 presents visualization of AC under the ultrasonic horn tip (UH)

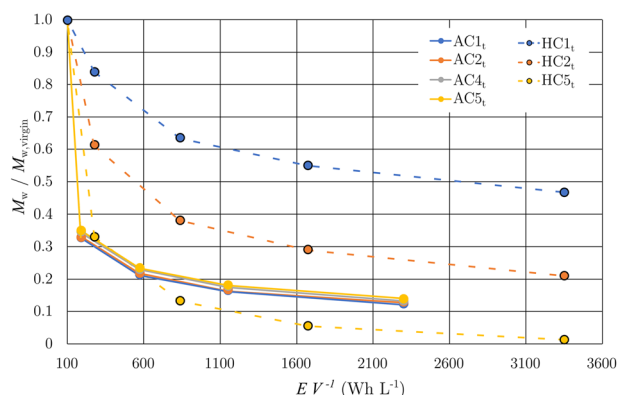


Fig. 5 Energy comparison between time dependent AC and HC treatment of PVOH. AC (solid lines) and HC (dashed lines) treatment for time dependent PVOH degradation. Coloured bullets (AC) and coloured bullets with black line strokes (HC) represent sampling times at 5, 15, 30, and 60 min. Results are presented as ratio between the weight-average molar masses of the treated samples and the virgin PVOH ($M_w/M_{w, \text{virgin}}$) as a function of the calculated energy input per sample volume ($E V^{-1}$).

(upper frames) and HC inside the cavitation chamber of the HC device (bottom frames). In addition, on the right side of Fig. 6 frequency spectra gained from a hydrophone for AC and HC are presented. In the case of AC, the frequency spectrum calculated from visualization is added to further support data collected from the pressure measurements.

High speed visualization under the UH tip (Fig. 6—upper frames) shows chaotic cavitation conditions, where two distinctive cavitation types can be observed: (1) a main cavitation region attached to the horn tip (contoured by a green line) and (2) individual gas/vapour bubbles, or bubble clusters detached from the main cavitation region (contoured by a yellow line). The main cavitation structure oscillates with frequencies around 2.5–3.3 kHz, corresponding to 1/8–1/6 of the driving frequency of the horn (20 kHz), while detached bubbles and bubble clusters oscillate with frequencies at around 17 kHz. Similar findings on subharmonic frequencies of the main cavitation structures were recorded and discussed by Žnidarčič et al.^{40,41} and are related to the UH geometry and not to the liquid properties. This “cavitation background” flashing—dispersed bubbles within the surrounding liquid are caused by pressure waves emitted from the UH tip. The characteristic frequencies are gained from frequency spectra based on hydrophone measurements and visualization analysis (Fig. 6 upper frames—right).

Visualization in the HC device (Fig. 6—bottom frames) shows stator grooves marked with a yellow line, while one of the rotor’s teeth is marked with a red line. The rotor turns counter-clockwise forming developed cavitation on each rotor tooth and in each stator groove. Since the number of rotor and stator teeth are the same (12) and the rotor turns with 10,000 rpm, the peak frequency signal from pressure pulsation measurements appears at 2 kHz and its harmonic at 4 kHz (Fig. 6 bottom frames – right). Cavitation on rotor teeth can be characterized as attached sheet cavitation with unstable rear-end shedding, resulting in detached cavitation cloud collapses. Inside the stator grooves rolling cavitation structures are formed, which collapse at the moment when the next rotor’s tooth pushes a high-pressure front with its

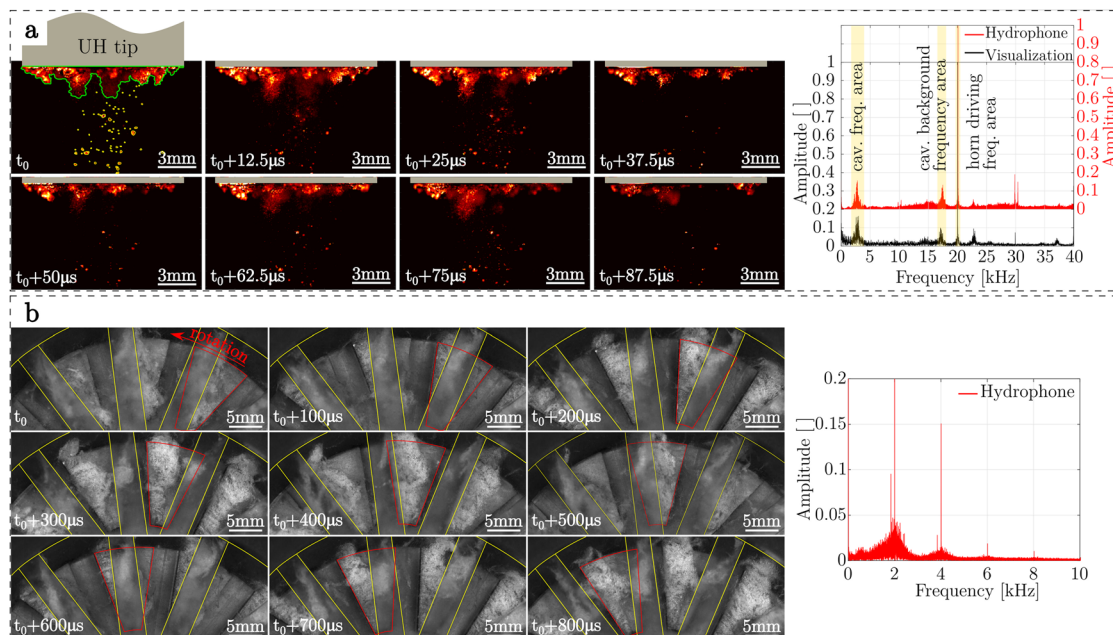


Fig. 6 High speed visualization and frequency analysis. High-speed visualization for **a** AC and **b** HC in distilled water. **a** AC cavitation time sequence captured under UH tip (left) with frequency spectrum based on visualization and pressure pulsation measurements (right). Contours in green and yellow lines in the first AC cavitation frame show two distinct cavitation types: attached to UH tip, and detached bubbles. **b** HC cavitation sequence in HC device (left) with frequency spectrum based on pressure pulsation measurements (right). In HC visualization frames a rotor tooth is marked by a red line and a stator tooth by a yellow line.

6 leading edge in the rotation direction. This forms simultaneously at all 12 teeth and grooves, resulting in intense cavitation conditions distributed through a much larger volume than in the case of AC.

Characterization of cavitation under selected experimental conditions

In addition to visualization in pure distilled water, characterization of AC and HC under selected experimental conditions (Table 1) was performed (Fig. 7). Since cavitation in a rotating HC device is too chaotic and it is extremely difficult to notice small differences between selected conditions, HC characterization was performed in a small Venturi device (test rig presented in detail in our paper⁴²). The alignment of the rotor and stator grooves resembles a Venturi-like geometry at each pair of teeth (Fig. 8: RGHC radial view), justifying the simplification of the experimental procedure to characterise cavitation. Using high speed photography and post processing image technique, results in form of averaged grayscale levels of recorded images (averaged for 0.1 s) are presented in color form, where blue indicates pure liquid and red pure vapour.

For both AC and HC, cavitation extent grows with higher temperature, which is due to higher vaporization pressure. Addition of H_2O_2 seems to have a minor effect at 25 and 60 °C in case of AC (Fig. 7E and F), while stronger deviations can be noticed in case of HC (Fig. 7E and F) compared to cavitation recorded in distilled water with PVOH (Fig. 7C and D). When comparing cavitation dynamics between distilled water (Fig. 7A and B) and water solution of PVOH with added H_2O_2 (Fig. 7E and F) significant differences for both cases, AC and HC, are observed.

DISCUSSION

Water-soluble polymers with fully carbon backbones (C-C) and pendant functional groups such as polyacrylamide, polyacrylic acid, or in the case of this study PVOH, can be degraded through C-C chain scission. This can be achieved by mechanical^{35–38,43,44} or chemical^{14,21,34,43,44} effects. Cavitation as a physical phenomenon includes both types: mechanical effects propagated by shear forces, shock waves, and microjets, all triggered by the collapse of cavitation bubbles, and chemical effects usually associated with

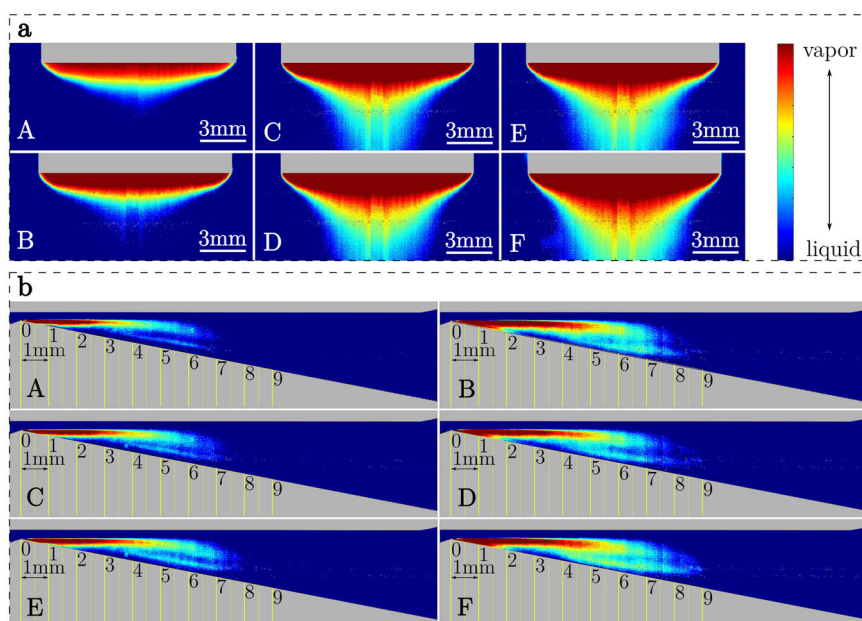


Fig. 7 Average cavitation extent under selected experimental conditions. Experimental conditions for **a** AC and **b** HC: A: H_2O (25 °C), B: H_2O (60 °C), C: H_2O (25 °C) + PVOH, D: H_2O (60 °C) + PVOH, E: H_2O (25 °C) + PVOH + H_2O_2 , F: H_2O (60 °C) + PVOH + H_2O_2 .

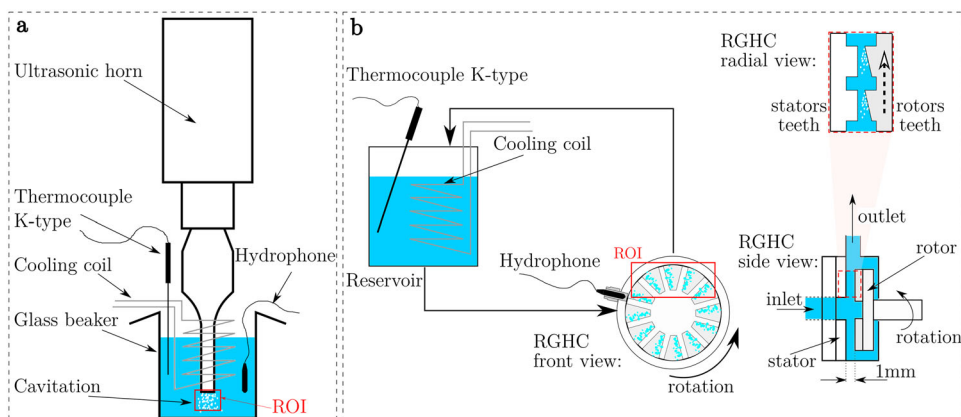


Fig. 8 Experimental set-up schemes for **a** AC and **b** HC. Red rectangular frame presents region of interest (ROI) captured by high-speed visualization. Positions of hydrophone, thermometer and cooling coil are schematically drawn.

OH formation triggered by local extreme temperatures or so-called hotspots. The intensity of the mechanical⁴⁵ and chemical effects⁴⁶ formed during cavitation may vary due to the operating conditions of the cavitation device and experimental conditions in terms of the properties and quality of the fluid⁴⁷. The results of our study clearly show that both AC and HC result in the degradation of PVOH, however differences were observed between the two processes. Although the basic mechanism of cavitation bubble formation and collapse is the same, there is a distinct difference between AC and HC in the behaviour of the random bubble clusters or cavitation clouds. This translates to mechanical and chemical effects of different intensity, which can lead to different results of the processes. We can see that after AC treatment under the investigated experimental conditions, the molar mass characteristics of PVOH do not differ significantly (Figs. 1 and 3). Slightly better PVOH degradation was always achieved at low PVOH concentrations. Results at higher concentrations are comparable except in the case of AC9, where a smaller MMA reduction compared to other AC cases (Fig. 1) could be attributed to the uniqueness of cavitation behaviour at around 60 °C^{48–50}. We believe that the higher effectiveness of AC at low PVOH concentration could relate to more extended coil conformation of high molar mass PVOH, which facilitates mechanical effects of AC. Our results are in agreement with other studies that used comparable PVOH concentrations of 0.1–3% (w/w)^{36–38}, concluding that in parallel with a higher PVOH concentration, the viscosity of the solution also increased, which consequently hindered the mechanical effects of AC. As molecules become less mobile and the velocity gradients around the collapsing bubbles are smaller, the degradation decreases in accordance with the viscosity increase³⁸. In addition to concentration, sample temperature is another important parameter affecting the degradation of chemical compounds with AC. As previously reported by Sun et al.²³, a lower experimental temperature seems to be beneficial for the degradation of PVOH by AC. Our results (Figs. 1 and 3) suggest a similar outcome, where MMA reduction is consistently higher at 25 °C (by a few kDa) compared to 60 °C. The observed unfavourable effect of higher temperature on PVOH degradation could be explained by the higher vapour pressure and thus larger and more numerous cavitation bubbles (Fig. 7—AC: B compared to A), which has a dampening effect on the intensity of cavitation, leading to lower mechanical degradation of PVOH. A similar degree of degradation obtained at 25 °C with the addition of MeOH (Fig. 1: AC3 and AC8) suggests that the degradation of PVOH during AC is predominantly due to mechanical effects, even though the presence of OH was experimentally confirmed by salicylic acid (SA) dosimetry (0.59 µg/mL of SA products determined) at these experimental conditions (Fig. 1: AC1*). However, these two experiments only confirmed that OH formed during cavitation do not play a role, but not that they never contribute to the degradation of PVOH. To confirm or deny this, an external oxidant was added to intensify the process. The experiments (Figs. 1 and 3) performed with the addition of H₂O₂ at 25 °C and 60 °C again gave PVOH with similar molar mass characteristics as the experiments without the addition, corroborating MeOH experiments and pinpointing mechanical effects as the main mechanism of PVOH degradation. The C–C scission due to mechanical effects is considered to be a non-random process³⁸, in which polymer chains are preferentially cleaved in the middle due to shear forces and shock waves^{23,36–38}, and larger molecules are degraded most rapidly³⁸. This can also be deduced from our SEC-RI chromatograms (Fig. 3), where the kinetics of chain scission slows down after the first 5 min of treatment, reaching a M_w of about 40 kg mol⁻¹, whereas the final M_w of 15.3 kg mol⁻¹ was reached after 60 min at 25 °C. The continuous decrease in MMAs and \bar{D}_M (Fig. 3) shows that the scission of the backbone does not occur randomly but predominantly in the central portion of the chains and does not proceed as fast as in the beginning once a certain

M_w is reached (40 kg mol⁻¹ in our case). The FTIR spectrum recorded for the experiment at 25 °C with the addition of H₂O₂ (Fig. 2a—AC7) shows no obvious increase in the intensity of the band due to the carbonyl group and no decrease in the intensity of the bands corresponding to stretching vibrations of O–H and C–O groups, once again pointing to mechanical effects as the main degradation mechanism. When mechanical effects are predominantly responsible for the scission of the main chain, only the C–C bonds of the polymer backbone are broken, resulting in alkyl and allyl functionalized PVOH chains as indicated by ¹H NMR.

On the other hand, HC treatment under different experimental conditions (Figs. 1 and 4) results in major differences, indicating that another mechanism is mainly responsible for PVOH degradation. Temperature can be excluded as an important degradation parameter, since the results (Fig. 1) at 25 °C and 60 °C without addition of H₂O₂ show comparable extent of PVOH degradation. Addition of MeOH (Fig. 1—HC3) indicates that OH might play a role in PVOH degradation, especially since the HC1* experiment (Fig. 1) showed that 0.50 µg/mL of SA products formed under these conditions. However, the FTIR spectra did not confirm this, as the characteristic band for the carbonyl group was not observed as a result of polymer oxidation (Fig. 2a—curves HC1 and HC4). However, this does not exclude the scission of the PVOH chains due to the OH but only that the concentration of PVOH terminal groups bearing a carbonyl group was too low to be detected by FTIR, since the MMA of PVOH are still high at this stage. The addition of H₂O₂ significantly improved the degree of PVOH degradation at both temperatures, implying that the degradation in these cases is caused by OH radicals in combination with mechanical effects. In studies investigating the degradation of PVOH by various AOP's, it was shown that OH, the common denominator of all, can effectively degrade PVOH and also lead to mineralization³⁴. When OH are responsible for the chemical scission of the C–C backbone, it can occur randomly anywhere along the polymer chain^{21,34}. The mechanism of the scission begins with the abstraction of hydrogen, followed by the formation of carbonyl group or carboxyl group formation from the –OH in the side chain finally leading to the formation of short polymer chains after the C–C bonds scission^{21,23}. This can be seen in the FTIR spectra in the case of HC2 and HC5 experiments (Fig. 2a), where raised carbonyl band suggests that OH were responsible for the chain scission. Similar to our study, Prajapat & Gogate⁴⁴ using HC showed enhanced degradation of polyacrylamide at lower concentrations, higher operating temperature and the addition of H₂O₂. They suggested that the polymer chains might become shorter due to both, mechanical and chemical effects of cavitation. However, since their FTIR spectra showed no chemical changes in the polymer structure, they concluded that if OH was responsible for breaking the polymer chains, it had no effect on its structure. Even though this study was performed for polyacrylamide and a direct comparison with PVOH is not possible, some general conclusions on the main mechanism involved during cavitation can still be drawn. The higher effectiveness of H₂O₂ addition in HC compared to AC might also be due to the high turbulence and consequently good mixing, which transports OH formed from H₂O₂ in the active cavitation zone more effectively into the bulk liquid. Since the entire sample is continuously transported through the cavitation chamber (Fig. 8), the probability of OH encountering a polymer chain is increased. Similarly, Prajapat and Gogate⁴⁴ concluded that the turbulence generated during HC provides better mixing, which facilitates the transport of OH from H₂O₂ into the bulk liquid and finally enhance polymer degradation. Our study shows that under the most extreme conditions (HC5_t: 60 °C and H₂O₂), the degradation of PVOH reaches 99% in 60 min, leading to M_w of 1.6 kg mol⁻¹ (Fig. 4, HC5_t). Additionally, the most pronounced changes in the FTIR spectrum (strong carbonyl band) were also observed for this experiment (Fig. 2a—HC5). Similar results were

obtained in our previous HC studies, in which the addition of H₂O₂ at 60 °C resulted in the highest removal of pharmaceuticals⁵¹, and the cavitation erosion between 30 °C and 100 °C at comparable HC conditions was most aggressive at about 60 °C⁵². We believe that in HC the combination of H₂O₂ and higher temperature strongly promotes the degradation of PVOH due to enhanced ·OH production, pinpointing chemical effects as the prevailing mechanism.

In terms of energy input (Fig. 5) more energy was applied to the samples with HC treatment, pointing to AC as more energy efficient treatment. But in the case of HC with addition of H₂O₂ and elevated temperature (HC5_v) lower molar masses were achieved with less energy, making this treatment as most energy efficient. AC as very localized and energy-intensive process delivers high amount of energy directly under the horn tip, where cavitation occurs. This area represents an active zone (about 125 mm³ or 0.25% of the total sample in our study—Fig. 6), while the rest of the volume is a passive zone. At the beginning of the treatment, when the C-C chains are the longest, the effectiveness of cavitation (active zone) is most pronounced, which can be deducted from the observed high rate of polymer chain breakage in the first 5 min. However, this advantage diminishes with time after a certain chain length is reached. Once most chains break to the limiting length, longer chains are less likely to reach a point of high energy density and encounter cavitation events. The non-uniform distribution of chains of all lengths in the sample and their random mass transfer between the active and passive zones⁵³ leads to the observed decrease in the degradation rate of C-C chains. Similar to our results, others^{23,38} also observed that polymer chain degradation stops at a certain viscosity. They suggested that below a certain limiting viscosity or molar mass, the polymer chains are too short to be affected by ultrasonic vibrations. A similar analogy can be drawn from cellulose fibre degradation, where Redlinger-Pohn et al.⁵³ suggested that fibres cannot be further shortened by AC after the limiting fibre length of 100 nm. On the other hand, in terms of energy density, HC is locally less intense than AC, since the supplied energy is distributed over a larger active zone. In this case the energy input is distributed over 2300 mm³, which corresponds to about 1% of the sample in comparison with AC. Therefore, in HC a single cavitation event is less likely to exceed the energy threshold to break a bond of the polymer chain mechanically.

Considering other experimental conditions, the limited AC active volume and non-uniform mixing are also likely the reasons why the results do not show improvement by the addition of H₂O₂ (Figs. 3 and 5). The ·OH should form from H₂O₂ under the influence of AC for the oxidant to have a pronounced effect. However, if the concentration of H₂O₂ is too high, it may start to act as a scavenger of the formed ·OH, reducing the effect⁵¹. Moreover, the transport of ·OH into the bulk liquid (passive zone) is slower due to the limited active volume and the possible degradation of the remaining shorter chains by ·OH is slowed down. A similar effect was observed by Hamad et al.¹⁴ in the UV/H₂O₂ process. The constant decrease in MMAs and \bar{M}_w in the case of AC (Fig. 3) also shows that the chain scission occurs predominantly in the central portion of the chains, whereas in the case of HC the degradation mechanism seems to be more complex (Fig. 4). Since the chemical reactions between PVOH and ·OH take place randomly along the polymer chain^{14,21,34,43,44}, the degradation of polymer chains is independent of chain length. In fact, the greater the number of shorter chains, the greater the probability that each ·OH formed will encounter a polymer chain and initiate scission. For this reason, the scission process in HC progresses continuously and no limiting chain length was encountered as is the case in AC. We can see that the biggest difference in HC is seen in the \bar{M}_w values. When H₂O₂ is added to the sample, the \bar{M}_w value initially increases regardless of temperature and only starts to decrease after 5 min, which

suggests that scission of PVOH chains by ·OH occurs randomly, which is in line with the results of Hamad et al.¹⁴. Moreover, different degradation rates were observed in the experiments at 25 and 60 °C with the addition of H₂O₂ after 15 min. This may be due to two mechanisms: (i) at 60 °C, a larger amount ·OH of H₂O₂ is generated, which may enter the bulk phase and contribute to the degradation of PVOH, or (ii) the added H₂O₂ affected the cavitation conditions (Fig. 7F). As can be clearly seen in Fig. 7A, the observed cavitation is different from that in distilled water when PVOH and H₂O₂ are in solution at 60 °C. It cannot be excluded that the addition of H₂O₂ changed the cavitation dynamics by inducing chemical effects (·OH) and enhancing mechanical effects, which then contributed to a better degradation of PVOH.

This study shows that PVOH can be degraded by AC and HC. By manipulating the experimental conditions, a very high degree of PVOH degradation by HC can be achieved. The results indicate that mechanical effects predominate in the case of AC, while chemical effects seem to play the most important role in HC, especially when H₂O₂ is added. The mechanism responsible for the degradation of PVOH in the case of HC without addition of H₂O₂ is elusive, and further experiments should be performed to determine which mechanism, chemical or mechanical, is responsible for the observed degradation. Nevertheless, the achieved degradation of PVOH to very short oligomer chains is an important achievement, as low MMA oligomers can be more easily biodegraded in nature. As is indicated by the FTIR spectra in the case of HC, these oligomers are highly oxidized, which is generally a factor that increases reactivity and promotes biodegradation. This study can serve as a starting point for the degradation of other polymers that are perhaps more harmful and difficult to degrade, such as those that constitute microplastics. Another advantage of the very high degradation achieved with HC is that this type of device can be easily scaled up and integrated into current WWT systems as a pre- or post-treatment process, preventing or reducing the negative effects of PVOH in the environment. However, TOC and ecotoxicity studies should be conducted before the technology can be considered safe and used at pilot or industrial scale. These analyses would show in more detail the extent to which cavitation can mineralize PVOH and confirm that no undesirable or even toxic products have been formed.

METHODS

Reagents

High purity salicylic acid (SA) (≥99%), 2,3-dihydroxybenzoic acid (2,3-DHBA, 99%) and 2,5-dihydroxybenzoic acid (2,5-DHBA, 98%) were purchased from Sigma-Aldrich. 1 M HCl and methanol (LiChrosolv®) for liquid chromatography were purchased from Honeywell Fluka. Trifluoroacetic acid (99%, extra pure) was purchased by Acros Organics. A total of 30% H₂O₂ was purchased from Belinka Petrokemija. PVOH with a hydrolysis degree of 98% was purchased from Merck and used as received.

Acoustic and hydrodynamic cavitation set-ups

Experiments were performed at the Faculty of Mechanical Engineering, University of Ljubljana. Two different experimental set-ups (Fig. 8) were used to exploit and compare specific characteristics of AC and HC and describe their effects on degradation of water soluble PVOH.

Experimental set-up for AC (Fig. 8—left) consisted of an UH (Cole Palmer, 750 W) installed on a vertically moving rack and a cooling coil. A total of 20 kHz UH had a 12.7 mm tip diameter made of titanium alloy. Highest intensity (100%) of the selected UH was used to exploit the strongest and most destructive conditions for PVOH treatment. The constant temperature of the

sample during experiments was maintained by a cooling coil, which was connected to an external portable cooling device DuraChill CA03 with 1.28 kW of cooling capacity. The temperature was monitored with a submerged thermocouple K-type. Horn tip with the cooling coil was submerged into the 100 mL glass beaker and positioned 15 mm from its bottom.

For the HC test rig (Fig. 8—right) a rotation generator of HC was installed in a closed loop. It was firstly used and described by Stepišnik-Perdih et al.⁵⁴ but optimised for present experiments. Test rig consisted of a reservoir with a volume of approximately 1 L with a submerged cooling coil, connected to the external DuraChill CA03 cooling device, enabling constant working temperature of the sample. Temperature was monitored with thermocouple K-type, submerged in the reservoir. Rotor was driven with a 3-phase, 2 kW electric motor via belt multiplier to ensure rotational frequencies above 50 Hz. Rotational generator of HC has a double function and works as a cavitation generator and as a pump simultaneously, thus no additional circulation pump is needed. It consists of a rotor and stator facing each other in an axial direction with special geometry, designed to achieve highly turbulent flow, causing cavitation formation. Rotor and stator have grooves in radial direction, resulting in teeth like geometry. They both have 12 grooves with the difference that rotor's teeth have an inclination, thus when a rotor's tooth is passing a stator's tooth the geometry or the space between them mimics single side Venturi constriction. Diameter of the rotor is 50 mm with the gap between rotor's and stator's front plane set at 1 mm. The rotational speed of the rotor was set to 10,000 rpm, resulting in circumferential velocity of 26 m s⁻¹.

Cavitation characterization

To help with the explanation of the results and to explain the differences between AC and HC, cavitation characterisation was performed via high-speed visualization and pressure pulsation measurements in distilled water. Visualization was performed by high-speed camera Photron FastCam SA-Z at 80,000 and 100,000 fps and resolution of 640 × 360 and 640 × 256 pixels in 12-bit monochrome technique for AC and HC, respectively. The red rectangles marked for AC and HC on Fig. 8, indicate the region of interest (ROI) for the visualization. By using high power LED illumination, we were able to set the shutter time down to 1 μs, while the aperture stayed half open. Pressure pulsations were measured with hydrophone RESON TC-4013 at 500 kHz via National Instruments cDAQ 9222 measurement card.

To further help with the explanation of the results additional cavitation characterisation (ACC) experiments were performed, since our previous study⁴⁷ confirmed anomalies with cavitation development and dynamics when salicylic acid (SA) in different concentrations was added to the water. Surface tension was determined as one of the physical characteristics of the samples that influenced the observed changes the most. For this reason, we investigated what effects do PVOH (known for influencing the surface tension of samples), temperature and H₂O₂ and their combinations have on cavitation. In the case of AC the set up presented in Fig. 8—left was used. In the case of HC, the visualization was performed in another HC set up more appropriate for determination of cavitation characteristics in more detail. The setup is explained elsewhere⁴². In short, a Venturi microchannel was used as a test section, which was made of transparent acrylic glass to enable visualization of cavitation structures from various angles. Small gear pump was used to provide the circulation of the sample from the reservoir through the test section. This evaluation was performed on samples at experimental conditions used for AC1, AC2, AC4 and AC5 in the case of AC and HC1, HC2, HC4 and HC5 in case of HC (Table 1). Additionally for comparison and to determine whether PVOH plays an important role in cavitation dynamics, visualization was

also performed in distilled water at 25 °C and 60 °C without the addition of PVOH (Fig. 7).

To determine the amount of energy transferred from the AC and HC devices directly to the PVOH samples, we performed the following two measurements. In the case of AC calorimetric analysis was performed and resulted in a power input of 115 W. In the case of HC power input of 670 W was determined using power analyser (Norma 4000). To differentiate energy losses between the electric motor and the rotor, electric power without the mounted rotor was measured at rotating frequency of 10,000 rpm and subtracted from the total power of the HC generator. To compare the efficiency of AC and HC we calculated the energy requirements (ER) as the ratio between the energy input at selected treatment times and sample volumes (Fig. 5E V⁻¹). The ERs (Wh L⁻¹) for the operation of AC and HC were evaluated at the selected experimental conditions (Table 1).

To confirm the chemical effects of AC and HC, namely ·OH formation, separate salicylic acid (SA) dosimetry experiments were performed in distilled water. Detailed chromatographic conditions for the analysis of SA products (2,3-DHBA and 2,5-DHBA) are described elsewhere⁴⁷. Determination of 2,3-DHBA and 2,5-DHBA formation were performed at experimental conditions used for AC1* and HC1* (Table 1). A total of 1 mL of each sample was taken after 30 min for HPLC analysis. The results presented in this study are part of a different, not yet published paper, and are only used to help with the explanation of the observed results.

Experimental design

The overview of the investigated experimental conditions and the analysis performed regarding PVOH degradation and cavitation characterization are presented in Table 1. Experiments were systematically designed to explore which experimental conditions and to what extent, influence degradation of PVOH. The effects of concentration, temperature and addition of H₂O₂ were investigated. Sample volumes for AC and HC were 50 and 200 mL, respectively. The experiments were firstly performed with AC where two concentrations of PVOH were used, 1 and 2 g L⁻¹ (Table 1, experiments AC1-AC5 and AC6-AC10, respectively). Samples were always prepared right before the experiments by mixing PVOH at an elevated temperature (up to 70 °C) on a magnetic stirrer to facilitate its solubilisation. Room temperature of 25 °C and 60 °C were selected as the temperatures of interest. 60 °C was chosen since our previous investigations showed that at this temperature cavitation is most effective for pharmaceuticals removal with HC⁵¹, distinct cavitation dynamics under UH⁴⁸ and cavitation erosion aggressiveness peak in HC⁵². Much higher temperatures were not chosen since they could influence PVOH degradation. To investigate whether chemical or mechanical effects were predominant in PVOH degradation, very high concentration of H₂O₂ as an external source of ·OH was added to the samples right prior to the experiments. The selected concentration was the same for all experiments (1 mL of 30% H₂O₂ per 100 mL of sample) and was chosen since it was shown as effective in our previous study⁵¹. Of course, to achieve optimal results different H₂O₂ doses should be tested and the optimal determined but this was not in the scope of this study. To confirm or refute that ·OH are responsible for PVOH degradation, experiments with the addition of a known radical scavenger methanol (MeOH) were performed. For this purpose, we added 1 mL L⁻¹ of MeOH, as this concentration was proven efficient for scavenging⁵⁵ and did not affect cavitation dynamics. Some experiments were performed in parallels. In the case of AC the results did not deviate for more than 5%, whereas for HC they were below 33%, except in the case of HC5 where deviation was higher due to very low *M_w* values.

Since the AC6-AC10 results did not show a big influence of PVOH concentration on its degradation, HC experiments (Table 1:

HC1-HC5) were performed only with a lower concentration, 1 g L^{-1} . These 5 experiments were performed in the same way as for the AC (Table 1: AC1-AC5). All the AC and HC experiments were at first performed only at 30 min of treatment. Later selected representative experiments were chosen to obtain time dependent degradation of PVOH (Table 1: AC1_t, AC2_t, AC4_t, AC5_t, HC1_t, HC2_t and HC5_t). In these experiments, samples for further analysis were taken after 5, 15, 30 and 60 min of treatment.

To investigate whether H_2O_2 alone influences the degradation of PVOH, we performed two control experiments (Table 1: C1 and C2) without cavitation. Experiment C1 was performed with addition of H_2O_2 at 25°C , while experiment C2 was performed with addition of H_2O_2 at 60°C . For these experiments a concentration 1 g L^{-1} of PVOH was chosen. The experiments were performed in 100 mL of distilled water and were left on a laboratory magnetic stirrer overnight.

After the treatment the whole sample volume was retrieved and stored at 8°C in glass bottles for further analysis.

Sample preparation and analysis

The molar mass averages of the treated PVOH samples were determined by size-exclusion chromatography coupled with a multi-angle light scattering and refractive index detectors (SEC/UV-MALS-RI). The solution of virgin PVOH was heated to 80°C and gently stirred for 3 h before SEC measurement to dissolve the polymer on a molecular level, whereas the PVOH solutions treated with AC and HC were injected onto the column without additional pre-treatment. Molar mass characteristics of PVOH were determined by size-exclusion chromatography (SEC) coupled with a multi-angle light-scattering (MALS) photometer with 18 angles (DAWN HELEOS-II, Wyatt Technology Corporation, USA) and a differential refractive index (RI) detector (Optilab T-rEX, Wyatt Technology Corporation, USA). Separation of the PVOH samples was performed at room temperature in water with added NaNO_3 (0.1 M) and 0.02 w/v% NaN_3 using an Agilent 1260 HPLC chromatograph (Agilent Technologies, USA) and PolarGel-M ($7.5 \times 300 \text{ mm}$, $8 \mu\text{m}$) analytical column with precolumn (Agilent Technologies, USA). The nominal flow rate of the eluent was 0.8 mL min^{-1} . Sample concentrations and injected masses of samples on the column were typically 1 mg mL^{-1} and $100 \mu\text{g}$, respectively. Astra 7.3.1 software (Wyatt Technology Corp., USA) was used for data acquisition and evaluation.

FTIR transmittance spectra of dried PVOH samples were recorded on a FTIR spectrometer Spectrum One (Perkin-Elmer, Waltham, MA, USA) in an ATR mode in a spectral range from 650 to 4000 cm^{-1} with a 4 cm^{-1} spectral resolution.

^1H NMR spectra of dried PVOH samples were recorded at room temperature in $\text{DMSO}-d_6$ using a Bruker AVANCE NEO 600 MHz instrument (Bruker Corporation, USA). Chemical shifts (δ) are given in ppm relative to a DMSO residual peak.

DATA AVAILABILITY

The data that support the findings of this study are available from the corresponding author upon reasonable request.

Received: 4 November 2022; Accepted: 17 April 2023;

Published online: 28 April 2023

REFERENCES

- Jambeck, J. R. et al. Plastic waste inputs from land into the ocean. *Sci. (80-)*. **347**, 768–771 (2015).
- Pabortsava, K. & Lampitt, R. S. High concentrations of plastic hidden beneath the surface of the Atlantic Ocean. *Nat. Commun.* **11**, 4073 (2020).
- Priya, A. K. et al. Microplastics in the environment: Recent developments in characteristic, occurrence, identification and ecological risk. *Chemosphere* **298**, 134161 (2022).
- Lebreton, L. et al. Evidence that the Great Pacific Garbage Patch is rapidly accumulating plastic. *Sci. Rep.* **8**, 4666 (2018).
- Ahmed, R., Hamid, A. K., Krebsbach, S. A., He, J. & Wang, D. Critical review of microplastics removal from the environment. *Chemosphere* **293**, 133557 (2022).
- Liu, W. et al. A review of the removal of microplastics in global wastewater treatment plants: characteristics and mechanisms. *Environ. Int.* **146**, 106277 (2021).
- Yang, X., Man, Y. B., Wong, M. H., Owen, R. B. & Chow, K. L. Environmental health impacts of microplastics exposure on structural organization levels in the human body. *Sci. Total Environ.* **825**, 154025 (2022).
- Koelmans, A. A. et al. Risk assessment of microplastic particles. *Nat. Rev. Mater.* **7**, 138–152 (2022).
- Gigault, J. et al. Nanoplastics are neither microplastics nor engineered nanoparticles. *Nat. Nanotechnol.* **16**, 501–507 (2021).
- Huppertsberg, S., Zahn, D., Pauelsen, F., Reemtsma, T. & Knepper, T. P. Making waves: water-soluble polymers in the aquatic environment: An overlooked class of synthetic polymers? *Water Res.* **181**, 115931 (2020).
- Julinová, M., Vaňharová, L. & Jurča, M. Water-soluble polymeric xenobiotics – Polyvinyl alcohol and polyvinylpyrrolidone – And potential solutions to environmental issues: a brief review. *J. Environ. Manag.* **228**, 213–222 (2018).
- Xu, S. et al. Influence of the PVA fibers and SiO_2 NPs on the structural properties of fly ash based sustainable geopolymer. *Constr. Build. Mater.* **164**, 238–245 (2018).
- Rolsky, C. & Kelkar, V. Degradation of polyvinyl alcohol in us wastewater treatment plants and subsequent nationwide emission estimate. *Int. J. Environ. Res. Public Health* **18**, 6027 (2021).
- Hamad, D., Mehrvar, M. & Dhib, R. Experimental study of polyvinyl alcohol degradation in aqueous solution by UV/ H_2O_2 process. *Polym. Degrad. Stab.* **103**, 75–82 (2014).
- Lofty, J., Muhawenimana, V., Wilson, C. A. M. E. & Ouro, P. Microplastics removal from a primary settler tank in a wastewater treatment plant and estimations of contamination onto European agricultural land via sewage sludge recycling. *Environ. Pollut.* **304**, 119198 (2022).
- Sol, D., Laca, A., Laca, A. & Díaz, M. Approaching the environmental problem of microplastics: Importance of WWTP treatments. *Sci. Total Environ.* **740**, 140016 (2020).
- Alonso-López, O., López-Ibáñez, S. & Beiras, R. Assessment of toxicity and biodegradability of Poly(vinyl alcohol)-based materials in marine water. *Polymers* **13**, 3742 (2021).
- Fedorov, K. et al. Synergistic effects of hybrid advanced oxidation processes (AOPs) based on hydrodynamic cavitation phenomenon: a review. *Chem. Eng. J.* **432**, 134191 (2022).
- Bibi, N. et al. Development of zerovalent iron and titania (Fe^0/TiO_2) composite for oxidative degradation of dichlorophene in aqueous solution: synergistic role of peroxymonosulfate (HSO_5^-). *Environ. Sci. Pollut. Res.* **29**, 63041–63056 (2022).
- Sayed, M. et al. Solar light induced photocatalytic activation of peroxymonosulfate by ultra-thin Ti^{3+} self-doped $\text{Fe}_2\text{O}_3/\text{TiO}_2$ nanoflakes for the degradation of naphthalene. *Appl. Catal. B Environ.* **315**, 121532 (2022).
- Yan, Z. et al. Catalytic ozonation for the degradation of polyvinyl alcohol in aqueous solution using catalyst based on copper and manganese. *J. Clean. Prod.* **272**, 122856 (2020).
- Wang, Y., Wang, H., Jin, H., Zhou, X. & Chen, H. Application of Fenton sludge coupled hydrolysis acidification in pretreatment of wastewater containing PVA: Performance and mechanisms. *J. Environ. Manag.* **304**, 114305 (2022).
- Sun, W., Chen, L. & Wang, J. Degradation of PVA (polyvinyl alcohol) in wastewater by advanced oxidation processes. *J. Adv. Oxid. Technol.* **20**, 20170018 (2017).
- Benito, Y., Arrojo, S., Hauke, G. & Vidal, P. Hydrodynamic Cavitation As A Low-cost AOP For Wastewater Treatment: Preliminary Results And A New Design Approach. *WIT Trans. Ecol. Environ.* **80**, 495–503 (2005).
- Suslick, K. S., Eddingsaas, N. C., Flannigan, D. J., Hopkins, S. D. & Xu, H. Extreme conditions during multibubble cavitation: Sonoluminescence as a spectroscopic probe. *Ultrason. Sonochem.* **18**, 842–846 (2011).
- Chahine, G. L., Kapahi, A., Choi, J.-K. & Hsiao, C.-T. Modeling of surface cleaning by cavitation bubble dynamics and collapse. *Ultrason. Sonochem.* **29**, 528–549 (2016).
- Chahine, G. L. & Hsiao, C.-T. Modelling cavitation erosion using fluid-material interaction simulations. *Interface Focus* **5**, 20150016 (2015).
- Brennen, C. E. *Cavitation and Bubble Dynamics*. (Oxford University Press, 1995).
- Franc, J. P. & Michel, J. M. *Fundamentals of Cavitation*. (Kluwer Academic Publishers, 2004).
- Zupanc, M. et al. Effects of cavitation on different microorganisms: The current understanding of the mechanisms taking place behind the phenomenon. A review and proposals for further research. *Ultrason. Sonochem.* **57**, 147–165 (2019).

31. Kim, H., Koo, B., Sun, X. & Yoon, J. Y. Investigation of sludge disintegration using rotor-stator type hydrodynamic cavitation reactor. *Sep. Purif. Technol.* **240**, 116636 (2020).
32. Khanh Nguyen, V. et al. Review on pretreatment techniques to improve anaerobic digestion of sewage sludge. *Fuel* **285**, 119105 (2021).
33. Petkovšek, M. et al. A novel rotation generator of hydrodynamic cavitation for waste-activated sludge disintegration. *Ultrason. Sonochem.* **26**, 408–414 (2015).
34. Dong, Y., Bian, L. & Wang, P. Accelerated degradation of polyvinyl alcohol via a novel and cost effective heterogeneous system based on Na₂S₂O₈ activated by Fe complex functionalized waste PAN fiber and visible LED irradiation. *Chem. Eng. J.* **358**, 1489–1498 (2019).
35. Holkar, C. R., Jadhav, A. J., Pinjari, D. V. & Pandit, A. B. Cavitational driven transformations: a technique of process intensification. *Ind. Eng. Chem. Res.* **58**, 5797–5819 (2019).
36. Grönroos, A. et al. Ultrasonic depolymerization of aqueous polyvinyl alcohol. *Ultrason. Sonochem.* **8**, 259–264 (2001).
37. Harkal, U. D., Gogate, P. R., Pandit, A. B. & Shenoy, M. A. Ultrasonic degradation of poly(vinyl alcohol) in aqueous solution. *Ultrason. Sonochem.* **13**, 423–428 (2006).
38. Mohod, A. V. & Gogate, P. R. Ultrasonic degradation of polymers: effect of operating parameters and intensification using additives for carboxymethyl cellulose (CMC) and polyvinyl alcohol (PVA). *Ultrason. Sonochem.* **18**, 727–734 (2011).
39. Mori, Y., Honda, T., Lu, R., Hayakawa, N. & Miyakoshi, T. Ultraviolet degradation of poly(vinyl alcohol) used in restoration of historical and cultural properties. *Polym. Degrad. Stab.* **114**, 30–36 (2015).
40. Žnidarčič, A., Mettin, R., Cairós, C. & Dular, M. Attached cavitation at a small diameter ultrasonic horn tip. *Phys. Fluids* **26**, 023304 (2014).
41. Žnidarčič, A., Mettin, R. & Dular, M. Modeling cavitation in a rapidly changing pressure field – Application to a small ultrasonic horn. *Ultrason. Sonochem.* **22**, 482–492 (2015).
42. Podbevšek, D., Petkovšek, M., Ohi, C. D. & Dular, M. Kelvin-Helmholtz instability governs the cavitation cloud shedding in Venturi microchannel. *Int. J. Multiph. Flow* **142**, 103700 (2021).
43. Prajapat, A. L. & Gogate, P. R. Intensification of depolymerization of polyacrylic acid solution using different approaches based on ultrasound and solar irradiation with intensification studies. *Ultrason. Sonochem.* **32**, 290–299 (2016).
44. Prajapat, A. L. & Gogate, P. R. Intensified depolymerization of aqueous polyacrylamide solution using combined processes based on hydrodynamic cavitation, ozone, ultraviolet light and hydrogen peroxide. *Ultrason. Sonochem.* **31**, 371–382 (2016).
45. Dular, M. & Petkovšek, M. On the mechanisms of cavitation erosion - Coupling high speed videos to damage patterns. *Exp. Therm. Fluid Sci.* **68**, 359–370 (2015).
46. Petkovšek, M. et al. Rotation generator of hydrodynamic cavitation for water treatment. *Sep. Purif. Technol.* **118**, 415–423 (2013).
47. Zupanc, M. et al. Anomalies detected during hydrodynamic cavitation when using salicylic acid dosimetry to measure radical production. *Chem. Eng. J.* **396**, 125389 (2020).
48. Petkovšek, M. & Dular, M. Cavitation dynamics in water at elevated temperatures and in liquid nitrogen at an ultrasonic horn tip. *Ultrason. Sonochem.* **58**, 104652 (2019).
49. Ge, M., Zhang, G., Petkovšek, M., Long, K. & Coutier-Delgosha, O. Intensity and regimes changing of hydrodynamic cavitation considering temperature effects. *J. Clean. Prod.* **338**, 130470 (2022).
50. Ge, M., Petkovšek, M., Zhang, G., Jacobs, D. & Coutier-Delgosha, O. Cavitation dynamics and thermodynamic effects at elevated temperatures in a small Venturi channel. *Int. J. Heat Mass Transf.* **170**, 120970 (2021).
51. Zupanc, M. et al. Shear-induced hydrodynamic cavitation as a tool for pharmaceutical micropollutants removal from urban wastewater. *Ultrason. Sonochem.* **21**, 1213–1221 (2014).
52. Dular, M. Hydrodynamic cavitation damage in water at elevated temperatures. *Wear* **346–347**, 78–86 (2016).
53. Redlinger-Pohn, J. D. et al. Cavitation fibrillation of cellulose fiber. *Biomacromolecules* **23**, 847–862 (2022).
54. Stepišnik Perdih, T., Širok, B. & Dular, M. Influence of hydrodynamic cavitation on intensification of laundry aqueous detergent solution preparation. *Strojniški Vestn. - J. Mech. Eng.* **63**, 83–91 (2017).
55. Filipič, A. et al. Hydrodynamic cavitation efficiently inactivates potato virus Y in water. *Ultrason. Sonochem.* **82**, 105898 (2022).

ACKNOWLEDGEMENTS

We acknowledge the financial support from the Slovenian Research Agency (research project No. J7-1814 and J2-3044, research core funding No. P2-0401, P1-0208 and P2-0145).

AUTHOR CONTRIBUTIONS

M.P. designed and performed the experiments with cavitation, analysed and interpreted the results and contributed to the paper text. A.K. performed FTIR analysis and validation with results interpretation and contributed to the paper text. E.Ž. conceptualization, characterization methodology, results interpretation and writing—review & editing. A.Š. performed characterization of salicylic acid products—HPLC analysis and validation with results interpretation. M.Z. accepted the role of the leading author, performed the experiments with cavitation, analysed and interpreted the results and contributed to the paper text.

COMPETING INTERESTS

The authors declare no competing interests.

ADDITIONAL INFORMATION

Correspondence and requests for materials should be addressed to Ema Žagar or Mojca Zupanc.

Reprints and permission information is available at <http://www.nature.com/reprints>

Publisher's note Springer Nature remains neutral with regard to jurisdictional claims in published maps and institutional affiliations.



Open Access This article is licensed under a Creative Commons Attribution 4.0 International License, which permits use, sharing, adaptation, distribution and reproduction in any medium or format, as long as you give appropriate credit to the original author(s) and the source, provide a link to the Creative Commons license, and indicate if changes were made. The images or other third party material in this article are included in the article's Creative Commons license, unless indicated otherwise in a credit line to the material. If material is not included in the article's Creative Commons license and your intended use is not permitted by statutory regulation or exceeds the permitted use, you will need to obtain permission directly from the copyright holder. To view a copy of this license, visit <http://creativecommons.org/licenses/by/4.0/>.

© The Author(s) 2023